Journal of Hazardous Materials 186 (2011) 352–359

Contents lists available at ScienceDirect

Journal of Hazardous Materials

journal homepage: www.elsevier.com/locate/jhazmat

Characterization of Alizarin Red S binding sites and structural changes on human serum albumin: A biophysical study

Fei Ding[a], Wei Liu[a,b], Jian-Xiong Diao[a], Ying Sun[a,*]

[a] Department of Chemistry, China Agricultural University, No. 2 Yuanmingyuan Xi Road, Haidian District, Beijing 100193, China
[b] College of Economics & Management, China Agricultural University, Beijing 100083, China

ARTICLE INFO

Article history:
Received 25 May 2010
Received in revised form 29 October 2010
Accepted 1 November 2010
Available online 9 November 2010

Keywords:
Alizarin Red S
Human serum albumin
Protein unfolding
Fluorescence spectroscopy
Molecular modeling

ABSTRACT

Alizarin Red S (ARS), is a water-soluble, widely used anthraquinone dye synthesized by sulfonation of *alizarin*. In this report, the binding of ARS to human serum albumin (HSA) was characterized by employing fluorescence, UV/vis absorption, circular dichroism (CD), and molecular modeling methods. The data of fluorescence spectra displayed that the binding of ARS to HSA is the formation of HSA–ARS complex at 1:1 stoichiometric proportion. Hydrophobic probe 8-anilino-1-naphthalenesulfonic acid (ANS) was employed and elucidated that the dye was located in subdomain IIIA. This phenomenon corroborates the result of site-specific probe displacement experiments, which demonstrate the dye is at indole–benzodiazepine site (Sudlow's site II); and it is also consistent with guanidine hydrochloride (GuHCl) induced HSA unfolding studies and molecular modeling simulations. The features of the dye, which led to structural perturbations of HSA, have also been studied in detail by methods of UV/vis, CD and three-dimensional fluorescence spectroscopy.

1. Introduction

Alizarin Red S (ARS), 1,2-dihydroxy-9,10-anthraquinonesulfonic acid sodium salt is a water-soluble, anthraquinone dye gained from the sulfonation of *alizarin*, a natural dye obtained from madder and is known since third millennium B.C. [1]. ARS has been widely used in the textile industry, but it also enjoys other applications such as staining bones in mammalian embryos and skeletons in small invertebrate embryos. However, ARS is a recalcitrant and durable dye that is both mutagenic and carcinogenic [1].

It is well-known that the absorption, distribution, metabolism and excretion (ADME) of various ligands are strongly affected by the protein–ligand interactions in the blood plasma [2]. Characterization of the molecular basis of these interactions is studied by evaluating the binding parameters, such as binding constants, thermodynamic functions and specific binding sites, etc. which is essential to understand the interactions in the biological systems and processes. HSA is the most abundant protein in plasma, with a concentration of about 6.0×10^{-4} M and provides about 80% of the blood osmotic pressure [3,4]. HSA molecule is a single chain of 585 amino acid globular nonglycoprotein, which is composed of three homologous α-helical domains (I, II, III), and each domain contains ten helices, divided into a six-helix and a four-helix subdomains (A and B). The capability of HSA to bind aromatic and heterocyclic ligands is largely depend on the existence of two principal binding sites (i.e. Sudlow's site I and site II), which are located within specialized cavities in subdomains IIA and IIIA, respectively, as well as some minor sites (i.e. tamoxifen and digitoxin sites) [5,6]. Site I is known as the warfarin–azapropazone site, formed as a pocket in subdomain IIA, and it involves the sole tryptophan (Trp^{214}) of the protein. Site II is known as indole–benzodiazepine site and corresponds to the pocket of subdomain IIIA, the interior pocket comprises hydrophobic amino acid residues and the exterior presents two important amino acid residues (Arg^{410} and Tyr^{411}) [7].

As the major soluble protein components of the circulating system, HSA is responsible for distributing and metabolizing many endogenous and exogenous ligands such as fatty acids, bilirubin, metal ions, steroids, pharmaceuticals and several dyes [8–11]. The exceptional ability of HSA to interact with these ligands is attributed to the presence of multiple binding sites. Moreover, the affinity of binding between the ligand and the plasma protein can supply vital information on the pharmacological/toxicological actions, biotransformation, biodistribution, etc. of ligands, since it has been demonstrated that the distribution and free concentration of various ligands can be drastically changed as a result of their binding to HSA [12,13]. Consequently, the study on the interaction

Abbreviations: ARS, Alizarin Red S; HSA, human serum albumin; Trp, tryptophan; Arg, arginine; Tyr, tyrosine; Cys, cysteine; Phe, phenylalanine; Ser, serine; ANS, 8-anilino-1-naphthalenesulfonic acid; GuHCl, guanidine hydrochloride; MRE, mean residue ellipticity; CD, circular dichroism; S.D., standard deviation.

* Corresponding author. Tel.: +86 10 62737071; fax: +86 10 62737071.
E-mail address: sunying@cau.edu.cn (Y. Sun).

0304-3894/$ – see front matter © 2010 Elsevier B.V. All rights reserved.
doi:10.1016/j.jhazmat.2010.11.002

of ligand with serum albumin is of imperative and fundamental importance. Here, the interaction between ARS and serum albumin was further studied using fluorescence, UV/vis, CD and molecular modeling techniques. The results have been discussed on the binding constants, protein unfolding studies in the presence of GuHCl, the identification of specific binding sites, and the effect of ARS on the structural changes of HSA. In addition, the exhaustive binding location of ARS to HSA was also clarified via molecular modeling approach. These discussions can serve as assistances to better understand the impact of ARS on serum albumin structure and function.

2. Experimental

2.1. Materials

HSA (fatty acid free < 0.05%) and ARS used in this experiment were purchased from Sigma–Aldrich (St. Louis, MO, USA) and without further purification. All other reagents employed were of analytical grade and were obtained from Sigma–Aldrich. Deionized water was generated by a Milli-Q Plus water system from Millipore (Waltham, MA, USA). Tris (0.2 M)–HCl (0.1 M) buffer solution containing NaCl (0.1 M) was used to keep the pH of the solution at 7.4. Dilutions of the HSA stock (1.0×10^{-5} M) in Tris–HCl buffer solution were prepared immediately before use, and the concentration of HSA was determined spectrophotometrically using $E^{1\%}_{1\,cm}$ of 5.30 at 280 nm [14]. The stock solution (3.0×10^{-5} M) of ARS was dissolved in Tris–HCl buffer solution.

2.2. Methods

2.2.1. Steady state fluorescence measurements

Fluorescence measurements were executed with an F-4500 spectrofluorimeter (Hitachi, Japan) equipped with a 1.0 cm quartz cell and a thermostatic bath. The HSA concentration in all the experiments was 1.0×10^{-6} M. The excitation and emission slit widths were fixed at 5.0 nm. The excitation wavelength was set at 295 nm to selectively excite the Trp^{214} residue, and the emission spectra were recorded in the wavelength range of 290–450 nm. Tris–HCl buffer solutions of ARS in corresponding concentrations were subtracted from all measurements. The fluorescence intensities were corrected for absorption of the exciting light and reabsorption of the emitted light to decrease the inner filter effect using the relationship [15]:

$$F_{cor} = F_{obs} \times e^{(A_{ex}+A_{em})/2} \quad (1)$$

where F_{cor} and F_{obs} are the fluorescence intensities corrected and observed, respectively, and A_{ex} and A_{em} are the absorption of the system at the excitation and the emission wavelength, respectively. The fluorescence intensity utilized in this paper is the corrected intensity.

2.2.2. Site-specific probe

Binding location studies between ARS and HSA in the presence of four site markers (phenylbutazone, flufenamic acid, digitoxin, and hemin) were performed using the fluorescence titration method. The concentration of HSA and site markers were all stabilized at 1.0×10^{-6} M, then ARS was added to site markers–HSA mixtures. An excitation wavelength of 295 nm was selected and the fluorescence emission spectra of HSA were collected.

2.2.3. Hydrophobic probe displacement

In the first series of experiments, HSA concentration was kept fixed at 1.0×10^{-6} M, and ARS/ANS concentration was varied from 2.5 to 22.5×10^{-8} M, HSA fluorescence was measured (λ_{ex} = 295 nm, λ_{em} = 332 nm). In the second series of experiments, ARS was added to solutions of HSA and ANS held in equimolar concentrations (1.0×10^{-6} M), and the concentration of ARS was also varied from 2.5 to 22.5×10^{-8} M, the fluorescence of ANS was registered (λ_{ex} = 370 nm, λ_{em} = 465 nm).

2.2.4. Molecular modeling

Molecular modeling of the HSA–ARS interaction was operated on SGI Fuel Workstation. The crystal structure of HSA (entry codes 1HK4, resolution 2.4 Å) was downloaded from the Brookhaven Protein Data Bank (http://www.rcsb.org/pdb). The two-dimensional (2D) structure of ARS was downloaded from PubChem (http://pubchem.ncbi.nlm.nih.gov). The potential of the three-dimensional (3D) of HSA was assigned according to the AMBER force field with Kollman all-atom charges. The initial structure of ARS was generated by molecular modeling software Sybyl 7.3. The geometry of the molecule was subsequently optimized to minimal energy using the Tripos force field with Gasteiger–Hückel charges, and the Surflex docking program was applied to calculate the possible conformation of the ligand that binds to the protein [16].

2.2.5. UV/vis absorption spectra

UV/vis absorption spectra were recorded on a Lambda-25 double-beam spectrophotometer (Perkin-Elmer, USA) at room temperature in the range 200–300 nm using a quartz cell with 1.0 nm path length.

2.2.6. CD spectra

CD spectra were collected with a Jasco-810 spectropolarimeter (Jasco, Japan) using a 0.2 cm path length quartz cuvette. Measurements were taken at wavelengths between 200 and 260 nm with 0.1 nm step resolution and averaged over five scans recorded as a speed of 50 nm min^{-1}. All observed CD spectra were baseline subtracted for buffer and the results were expressed as mean residue ellipticity (MRE) in deg cm^2 $dmol^{-1}$ which is defined as

$$MRE = \frac{\theta_{obs}}{10 \times n \times l \times C_p} \quad (2)$$

where θ_{obs} is the CD in millidegree, n is the number of amino acid residues (585), l is the path length of the cuvette, and C_p is the HSA molar concentration. α-helical content was calculated on the basis of change of MRE values at 208 nm using the following equation as described by Greenfield and Fasman [17]:

$$\%\alpha\text{-helix} = \frac{MRE_{208} - 4000}{33,000 - 4000} \quad (3)$$

2.2.7. Three-dimensional fluorescence spectra

Three-dimensional fluorescence spectra were scanned under the following conditions: the emission wavelength was recorded between 200 and 500 nm, the initial excitation wavelength was set to 200 nm with increment of 10 nm, the number of scanning curves was 16, and other scanning parameters were identical to those of the fluorescence emission spectra.

3. Results and discussion

3.1. Dye–HSA binding determination

3.1.1. Steady state fluorescence

Fluorescence gives information about the accessibility of ligands to the fluorophores of protein. Changes in the fluorescence emission spectra of fluorophores are common in response to protein conformational changes, subunit association, substrate binding, or denaturation [15]. Fig. 1 shows the raw data for quenching of HSA

Table 1
Quenching constants and binding parameters for the interaction of ARS with HSA.

T (K)	K_{SV}[a] ($\times 10^5$ M^{-1})	k_q ($\times 10^{13}$ M^{-1} s^{-1})	K_b ($\times 10^5$ M^{-1})	n	ΔG° (kJ mol^{-1})
298	4.86	4.86	4.613	0.99	−32.31
302	4.36	4.36	3.945	0.99	−32.35
306	3.67	3.67	3.221	0.98	−32.27
310	3.01	3.01	2.449	0.98	−31.98

[a] The mean value of three independent experiments with standard deviation (S.D.) ± 0.12–0.95%.

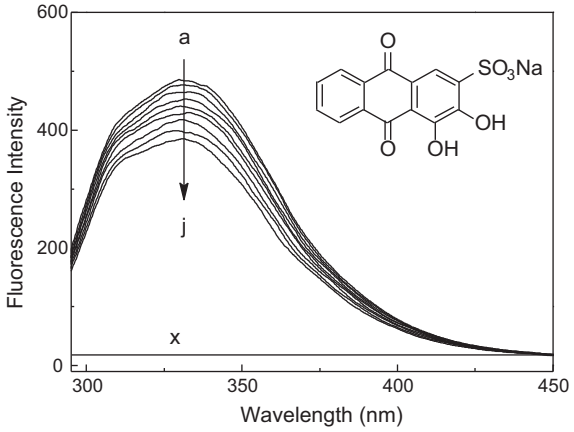

Fig. 1. Fluorescence emission spectra of HSA concentration 1.0×10^{-6} M in Tris–HCl buffer, pH 7.4, T = 298 K in the absence and presence of ARS following an excitation at 295 nm. The ARS concentration was 0, 2.5, 5.0, 7.5, 10.0, 12.5, 15.0, 17.5, 20.0, 22.5×10^{-8} M from (a) to (j), (×) 22.5×10^{-8} M ARS. The inset corresponds to the chemical structure of ARS.

Trp^{214} residue fluorescence at pH 7.4 with the addition of ARS, and this caused a gradual decrease in the fluorescence emission spectra of HSA, without changing the emission maximum and shape of the peaks. These observations indicated that there were interactions between ARS and HSA [18]. To further elucidate the fluorescence quenching mechanism, Stern–Volmer equation was utilized for the fluorescence data process [19]:

$$\frac{F_0}{F} = 1 + K_{SV}[Q] = 1 + k_q \tau_0 [Q] \quad (4)$$

In Eq. (4), F_0 and F are the fluorescence intensities in the absence and presence of quencher, respectively, K_{SV} is the Stern–Volmer quenching constant, k_q is the bimolecular quenching constant, τ_0 is the lifetime of the fluorophore in the absence of quencher (10^{-8} s [15]), and [Q] is the concentration of quencher. K_{SV} was acquired from the slope of linear regression of a plot of F_0/F *versus* [Q]. Fig. 2 displays the Stern–Volmer plot for the HSA fluorescence quenching by ARS, the Stern–Volmer plot does not show deviation from linearity toward the *y*-axis at high ARS concentrations. On the contrary, it exhibits a good linearity and the quenching constants K_{SV} and k_q were collected in Table 1. The value of k_q is 1.0×10^3-fold higher than the maximum value for diffusion-controlled quenching in water (~10^{10} M^{-1} s^{-1} [15]), which implies that there was a non-fluorescent complex formation between ARS and HSA (static mechanism).

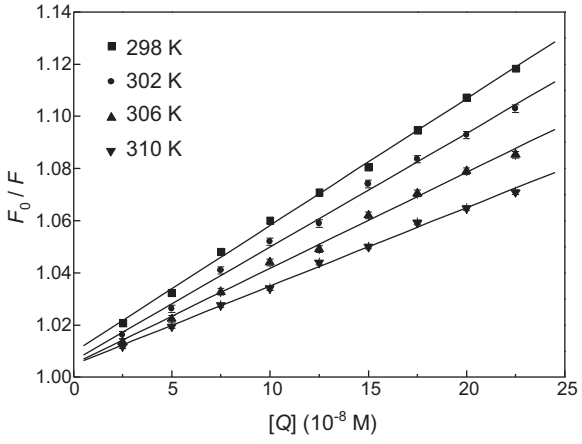

Fig. 2. Stern–Volmer plots describing Trp quenching of HSA in the presence of different concentrations of ARS. Each data point was the mean of three independent observations ± S.D. ranging 0.1–0.2%.

3.1.2. Binding analysis

When ligand molecules that binds independently to a set of equivalent sites on a macromolecule, the equilibrium between free and bound molecules is given by the following equation [20]:

$$\log \frac{F_0 - F}{F} = \log K_b + n \log[Q] \quad (5)$$

where F_0 and F are the fluorescence intensities in the absence and presence of quencher, K_b and n are the binding constant and the number of binding site, [Q] is the concentration of quencher. Hence, Eq. (5) was applied to determine K_b and n by a plot of $\log(F_0-F)/F$ *against* log[Q], and the standard free energy change ΔG° of the dye binding to HSA was calculated from the relationship:

$$\Delta G^\circ = -RT \ln K_b \quad (6)$$

where K_b is the binding constant and R is the gas constant, the values of K_b, n, and ΔG° thus determined and also listed in Table 1. It was found that the binding constant K_b decreased with an increase in temperature, resulting in the destabilization of the HSA–ARS complex. Furthermore, the number of binding site n approximately equal to 1 indicated there is merely a single binding site in HSA molecule for ARS [21]. The results of this aspect are discussed in the next section.

3.1.3. Stoichiometric analysis

The stoichiometry of HSA–ARS interaction was determined by the method of Job's plot analysis (also known as the method of continuous variation) [22]. It is a very useful method for the characterization of complex formed by an interaction of two species. In this method, the molar fractions of ARS and HSA were varied while keeping the total concentration (c(dye) + c(HSA)) constant, the fluorescence intensity was measured ($\Delta F = F_{HSA} - F_{dye+HSA}$) and plotted *versus* the ARS molar fraction (X_{Ligand}). The results showed that the cross point between the two straight lines occurs at a molar fraction (X_{dye}) around 0.5, which suggests that the stoichiometric proportion of HSA:ARS at 298 K and pH 7.4 is 1:1 (Fig. 3).

3.2. Allocation of binding site

3.2.1. Effect of guanidine hydrochloride (GuHCl)

After finding the interaction between HSA and ARS, the experiment of GuHCl induced unfolding of HSA was employed to characterize the ARS binding location in HSA molecule. Ahmad et al. [23] examined the GuHCl induced unfolding of HSA and found that at 1.4 M GuHCl, only domain III is completely unfolded, the presence of a molten globule-like state of domain III around 1.8 M GuHCl. This

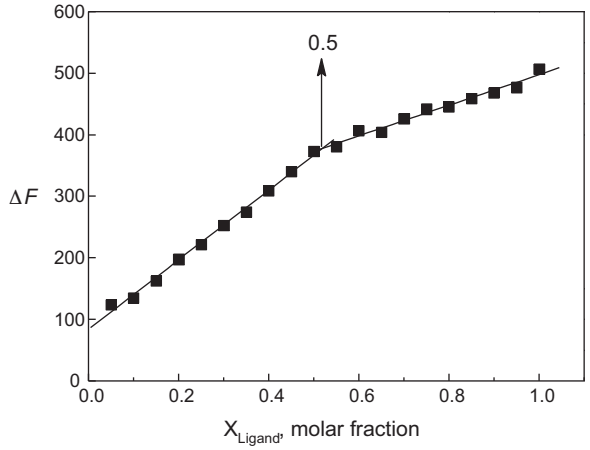

Fig. 3. Job's plot of fluorescence intensity changes as a function of molar fraction of ARS, pH 7.4, $T = 298$ K.

conclusion has been verified by Galantini et al. [24], who exploited a small-angle X-ray scattering and light scattering methods to discuss the unfolding pattern of fatted and defatted HSA, in denaturing conditions induced by GuHCl. In this work, samples of different GuHCl concentrations were titrated with 6.0 M GuHCl stock solution and Tris–HCl buffer of pH 7.4. The final solution mixture was incubated with 1.4 M and 1.8 M GuHCl for 12 h at room temperature before fluorescence measurements. Based on Eq. (5), when the domain III is entirely unfolded, the binding constant between HSA and the dye drastically reduced ( ), particularly at 1.8 M GuHCl ( ), the molten globule-like state. Therefore, the outcomes of the denaturation of HSA induced by GuHCl strongly evidenced that unfolding of domain III remarkably affects the binding of ARS to HSA, namely, the dye bind predominantly to the region of HSA.

3.2.2. Hydrophobic probe ANS

Fluorescence dye 8-anilino-1-naphthalenesulfonic acid (ANS) is sensitive to microenvironmental changes and can examine the structure and interactions of proteins, so it has been utilized to provide information on all the hydrophobic binding sites in HSA molecule [25]. In order to further understand the nature of the interaction between ARS and HSA, binding studies were carried out in the presence of ANS under identical conditions. The relative fluorescence intensity (F/F_0) *versus* ligand concentration ([Ligand]) plots is shown in Fig. 4. At a ligand concentration of 22.5×10^{-8} M,

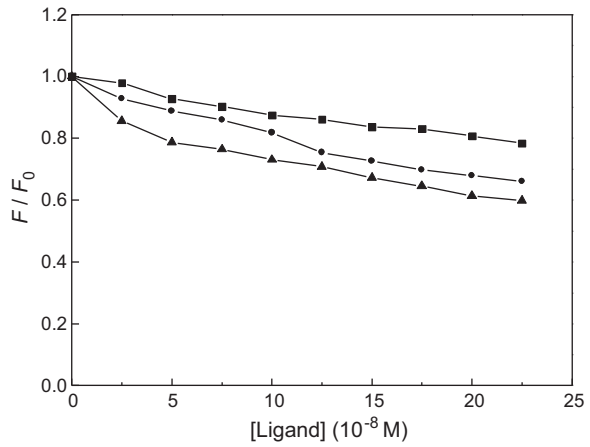

Fig. 4. Fluorescence quenching profile of HSA and HSA–ANS mixture. Binding isotherm of ARS (■) and ANS (●) induced quenching of HSA fluorescence and quenching of HSA–ANS mixture fluorescence by ARS (▲); pH 7.4, $T = 298$ K.

Table 2
The binding constants of competitive experiments of HSA–ARS system.

Site marker	K'_b [a] ($\times 10^5$ M^{-1})	R [b]
Phenylbutazone	4.667	0.9993
Flufenamic acid	0.5943	0.9996
Digitoxin	4.131	0.9985
Hemin	4.083	0.9995

[a] The mean value of three independent experiments with S.D. ± 0.8–2.8%.
[b] R is the correlation coefficient.

both ARS and ANS had a similar quenching effect on HSA fluorescence, which indicated that ARS and ANS are bound to the same hydrophobic cavity of HSA.

The dye, ARS, when added to HSA–ANS mixture, can compete with ANS for hydrophobic portion, and therefore the fluorescence intensity should decrease (Fig. 4). The reason is that ANS is essentially non-fluorescent when in aqueous solution, but it will become highly fluorescent in non-polar solvents or when it is bound to proteins [26]. Furthermore, Stryer first reported [27] that the quantum yield of ANS is about 0.002 in aqueous buffer, but near 0.4 when bound to albumin, with almost no contribution to the unbound probe, and the use of ANS is proposed as a hydrophobic probe for the study of their environment polarity and the hydrophobic site in a given protein. Although still partly controversial, consensus exists today that there are four hydrophobic binding sites for ANS association with HSA, but preferentially at a site in subdomain IIIA [14,28–30]. In this work, ANS strongly quenches the fluorescence of HSA, indicates that the binding site for ANS is in this high-affinity site (subdomain IIIA). Also, approximately 40.13% displacement of ANS fluorescence confirms that ARS and ANS share a common site in HSA, that is, Sudlow's site II (subdomain IIIA).

3.2.3. Site-specific probe

In order to further identify ARS binding sites on HSA, site marker competitive experiments are conducted by using drugs specifically bind to a know site or region on HSA. The first crystallographic analyses of HSA [31] revealed that it comprises three structurally homologous domains (I, II, III): I (residues 1–195), II (196–383), III (384–585), each of which is composed of two subdomains (A and B) and is stabilized by 17 disulfide bonds and 1 free thiol at Cys^{34}. HSA is known to contain two major binding regions for ligands, namely, Sudlow's site I and site II. Site I shows affinity for bulky heterocyclic anion with a negative charge localized in the middle of the molecule [7]. Drugs binding in site I include warfarin, indomethacin, phenylbutazone and azapropazone. While ligands bind to site II are aromatic carboxylic acids with negatively charged acidic group at the end of the molecule, such as ibuprofen, diazepam, flufenamic acid and propofol [32].

Shortly afterwards Sjöholm et al. [33] pointed out that digitoxin binding in HSA is sovereign of Sudlow's site I and II, and perch on what was nominated as site III. In this research, the competitors used included phenylbutazone, a characteristic marker for site I, flufenamic acid for site II, digitoxin for site III, and hemin for domain I. According to the experimental protocol, the binding constants in the presence of the site markers were evaluated exploiting Eq. (5). The K'_b values are obtained directly from the intercept of Eq. (5) for all systems which have a linear graphic are summarized in Table 2. The results signify that the binding constant of the HSA-flufenamic acid system was almost 12.88% of that without flufenamic acid, while the other HSA–site marker system has only a small difference. The observation verifies that the binding of ARS to HSA is chiefly located within domain III, Sudlow's site II. This result corroborates with the GuHCl induced denaturation of HSA and ANS displacement experiments, and is also consistent with molecular modeling simulations below.

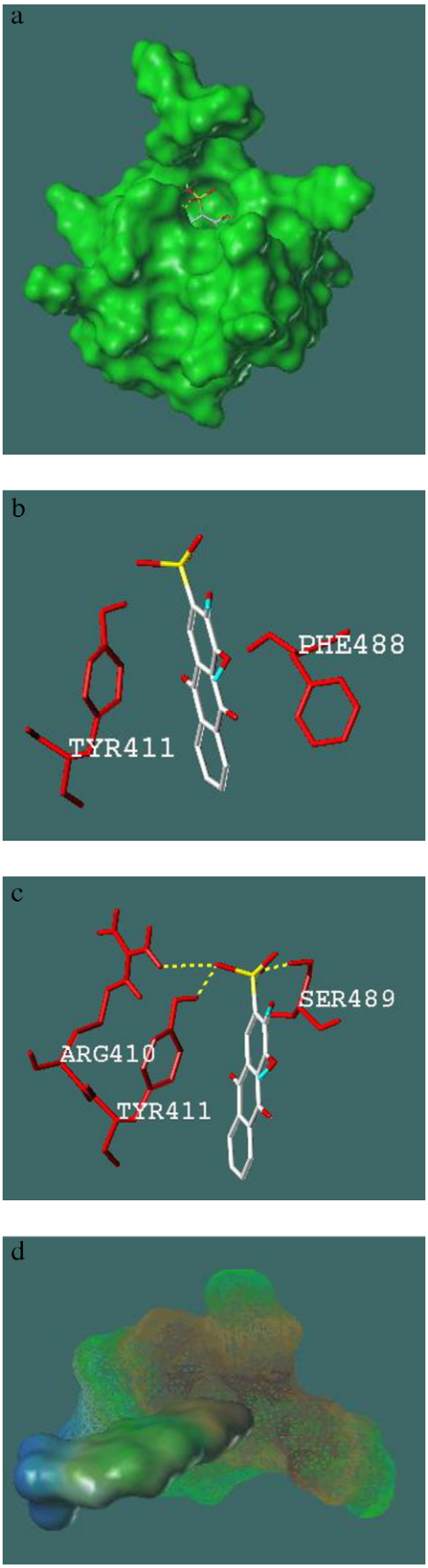

3.3. Molecular modeling

To obtain more insight into the ARS interaction with HSA, molecular modeling simulations were applied to examine the binding of ARS at the active site of HSA. The best docking energy result is shown in Fig. 5(A). It can be seen that ARS was situated within subdomain IIIA in Sudlow's site II formed by six-helices, and Tyr^{411}, Phe^{488} residues terminal benzene ring can make hydrophobic interactions with anthracene ring of ARS (Fig. 5(B)). The interactions between ARS and HSA are not exclusively hydrophobic interactions in nature because there are three polar residues (Arg^{410}, Tyr^{411} and Ser^{489}) in the vicinity of the bound ligand, acting a considerable role in stabilizing ARS by hydrogen bonds interactions (Fig. 5(C)). For example, Arg^{410} is in an appropriate position involved in making hydrogen bonds with oxygen atom of the sulfo group side chain in ARS. The phenomenon manifested that the formation of hydrogen bonds acts as an "anchor", which extremely determines the three-dimensional space position of ARS in the subdomain IIIA, and stimulates the hydrophobic interactions of the anthracene ring with the side chain of HSA [34]. In addition, there is a hydrophobic cavity at the bottom of subdomain IIIA, and the anthracene ring of ARS also has a tendency to conjugate with the cavity via hydrophobic interactions (Fig. 5(D)). The above docking results and analyses certify the denaturation of HSA through GuHCl and fluorescence probes studies, which place the ARS molecule at subdomain IIIA, and suggest structural changes of HSA upon interaction with ARS.

It is noteworthy that HSA contains a single Trp^{214} residue in domain II, in order to acquire information regarding the microenvironment of this residue, fluorescence emission spectra were measured after excitation at 295 nm (to favor Trp excitation) [15]. In this study, the GuHCl induced unfolding of HSA, fluorescence probes studies and molecular modeling results demonstrate the binding of ARS to HSA principally situated within subdomain IIIA. The observed phenomena could be explained with the fact that subdomain IIA and IIIA share a common interface, the helices of subdomain IIIA being very closely to those of subdomain IIA, and ARS in Sudlow's site II could be adjacent to Trp^{214} than in subdomain IIA [4,35], consequently, this finding provided a good structural basis to explain the very efficient fluorescence quenching of Trp^{214} emission in the presence of other ligand which has analogous configuration with ARS.

3.4. Alterations of HSA secondary structure

3.4.1. UV/vis absorption spectra

UV/vis absorption measurement is a very simple method and applicable to explore the structural changes. Fig. 6 shows the UV/vis absorption spectra of HSA from 200 to 300 nm in Tris–HCl buffer in the presence of various ARS concentrations. As can be seen from Fig. 6, ARS was almost non-UV absorption under the presence conditions. HSA has a strong absorption peak at 208 nm, which represents the content of α-helical structure of HSA, and the absorbance of HSA at 208 nm decreased with the addition of ARS. The reason may stem from the interac-

Fig. 5. Molecular modeling of ARS bound HSA. Panel (A) shows docked ARS into HSA at subdomain IIIA. Subdomain IIIA of HSA, represented in surface colored in green, to ARS, represented in stick, colored as per the atoms. Panels (B) and (C) depict the amino acid residues involved in binding of ARS. The residues of HSA around ARS have been displayed in red color. Grey color stick model shows the ARS molecule. The hydrogen bonds between HSA and ARS represented using yellow dash line. Panel (D) displays the vertical view of HSA subdomain IIIA. Subdomain IIIA, represented in surface colored in green, to ARS, represented in surface colored in khaki. (For interpretation of the references to color in this figure legend, the reader is referred to the web version of the article.).

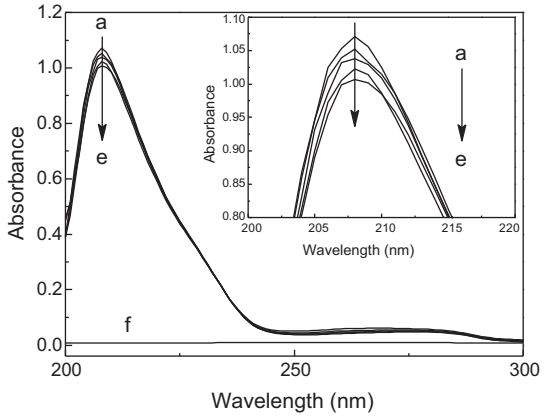

Fig. 6. UV/vis absorption spectra of HSA. HSA concentration was at 1.0×10^{-6} M (a) and ARS concentration for HSA–ARS system was at 2.5, 5.0, 7.5, 10.0×10^{-8} M (b)→(e); A concentration of 2.5×10^{-8} M ARqS (f) was used for ARS only; pH 7.4, T = 298 K.

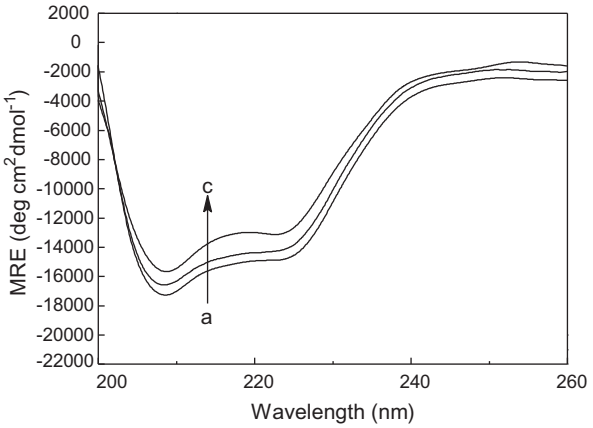

Fig. 7. CD spectra of the HSA–ARS mixture. (a) 1.0×10^{-6} M HSA, (b) 1.0×10^{-6} M HSA = 1.0×10^{-6} M ARS; (c) 1.0×10^{-6} M HSA = 2.0×10^{-6} M ARS; pH 7.4, T = 298 K.

tion between HSA and ARS, and led to the structural alterations of HSA.

3.4.2. CD spectra

To further investigate the structural changes of HSA were associated with the ARS, CD spectra of HSA were recorded with and without the addition of ARS. Fig. 7 expresses raw CD spectra from the range of 200–260 nm for the HSA samples in the absence and presence of ARS. The CD spectra of HSA exhibited two negative bands in the UV region at 208 and 222 nm, which are typical features of an α-helical protein structure [36]. A reasonable explanation is that the negative peaks between 208 and 209 nm and 222 and 223 nm are both contributed by $n \rightarrow \pi^*$ transition for the peptide bond of α-helix [17]. Moreover, the CD spectra of HSA in the presence and absence of ARS were similar in shape, which interprets that the structure of HSA was also predominantly α-helix. The addition of ARS to HSA induced only a decrease with the negative Cotton effect and without any evident shift of the peaks, revealed

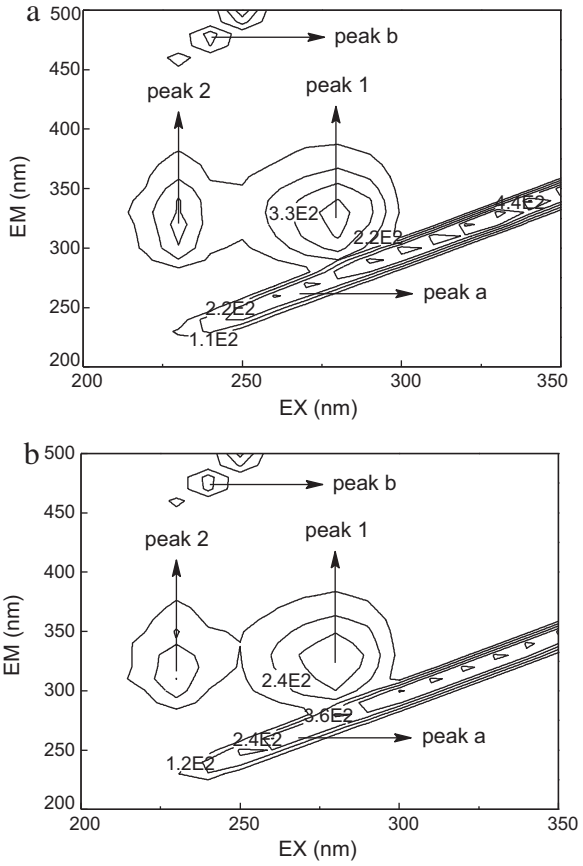

Fig. 8. Three-dimensional fluorescence contour map of HSA (a) and the HSA–ARS mixture (b). (a): c(HSA) = 1.0×10^{-6} M, c(ARS) = 0; (b): c(HSA) = 1.0×10^{-6} M, c(ARS) = 5.0×10^{-8} M; pH 7.4, T = 298 K.

the slight changes in the protein secondary structure. The α-helical content of HSA was calculated from Eq. (3), and the results displayed a reduction of α-helical structures from 45.37% to 40.67% and 36.93% at a molar ratio of HSA to ARS of 1:1 and 1:2, respectively, illustrating the destabilization of HSA secondary structure on HSA–ARS association reaction [37].

3.4.3. Three-dimensional fluorescence spectra

Additional evidence of structural changes of HSA upon the addition of dye was verified by three-dimensional fluorescence spectroscopy. Fig. 8 shows the three-dimensional fluorescence contour map obtained of HSA at pH 7.4 with the addition of ARS as quencher, and Table 3 summarizes the corresponding characteristic parameters. Peak a ($\lambda_{ex} = \lambda_{em}$) is the Rayleigh scattering peak, peak b ($\lambda_{em} = 2\lambda_{ex}$) is the second-order scattering peak, and the fluorescence intensities of the two peaks increased with the addition of ARS. The reason is that a HSA–dye complex come into being after the addition of dye, it makes the diameter of the macromolecule increased, and therefore leads to an enhanced scattering effect. Peak 1 (λ_{ex} = 280.0 nm, λ_{em} = 329.0 nm) chiefly reveals the spectral characteristic of Tyr and Trp residues, because HSA is excited at

Table 3
Three-dimensional fluorescence spectral characteristic parameters of HSA and HSA–ARS mixture.

Peaks	HSA			HSA–ARS		
	Peak position $\lambda_{ex}/\lambda_{em}$ (nm/nm)	Stokes $\Delta\lambda$ (nm)	Intensity F	Peak position $\lambda_{ex}/\lambda_{em}$ (nm/nm)	Stokes $\Delta\lambda$ (nm)	Intensity F
Rayleigh scattering peaks	250/250 → 350/350	0	383.0 → 536.6	250/250 → 350/350	0	460.5 → 643.7
Fluorescence peak 1	280.0/329.0	49.0	488.7	280.0/329.0	49.0	465.4
Fluorescence peak 2	230.0/320.0	90.0	389.6	230.0/320.0	90.0	346.2

280 nm, it mainly shows the intrinsic fluorescence of Tyr and Trp residues, and the phenylalanine (Phe) residue fluorescence can be negligible [15]. Peak 2 (λ_{ex} = 230.0 nm, λ_{emv} = 320.0 nm) is primarily caused by the transition of $P \rightarrow P^*$ of HSA, and it displays the fluorescence spectral behavior of the polypeptide chain backbone structure C=O. Analyzing from the intensity changes of peak 1 and 2, they decreased obviously but to a different extent: the intensity of peak 1 has been quenched of 4.77%, while peak 2 of 11.14%. The decrease of the intensity of the two peaks in combination with the UV/vis and CD results indicated that the binding of ARS to HSA induced the slight unfolding of the polypeptide chain of protein, resulted in the structural changes of HSA and increased the exposure of some hydrophobic portions which were previously buried [38]. From the above results, it was apparent that the effect of ARS to HSA aroused some microenvironmental and structural changes of the protein.

4. Conclusions

In a word, the upshots of this task evidently declare that the binding of ARS to HSA was the formation of HSA–ARS complex with a binding constant of 10^5 M^{-1}, and having the stoichiometry of 1:1. Based on GuHCl evoked HSA unfolding experiments, domain III was assigned the high-affinity site for the binding of ARS on HSA. This was confirmed by ANS displacement, site-specific probes, and molecular modeling studies, which found that flufenamic acid, as marker ligand of Sudlow's site II (indole–benzodiazepine site), competed with ARS for this site. Into the bargain UV/vis, CD and three-dimensional fluorescence spectra suggested that the binding of ARS to HSA caused some structural changes of HSA. Even though our works do not correlate directly *in vivo* bioassay, it lends significant insight to the interactions of the protein with toxic anthraquinone dye. Since HSA is the key carrier for ligands in blood, under physiological conditions, to transport this toxic compound to the target tissue, where it elicits its toxicological action.

Acknowledgements

We thank Dr. Li Zhang of Key Laboratory of Pesticide Chemistry and Application Technology, Ministry of Agriculture, Department of Applied Chemistry, China Agricultural University, for her priceless assistance in molecular modeling. Thanks are also due to Dr. Li Zhang of Department of Chemistry, China Agricultural University, for her constant support during the CD measurements. This work was performed under the auspices of the Postgraduate Research and Innovation Project, China Agricultural University.

References

[1] Q.G. Jiang, Y.J. Ji, Y.X. Chang, Handbook on Toxic Pollutant in Environment Analytical Chemistry, first ed., Chemical Industry Press, Beijing, 2004.
[2] P. Brunmark, S. Harriman, P.L. Skipper, J.S. Wishnok, S. Amin, S.R. Tannenbaum, Identification of subdomain IB in human serum albumin as a major binding site for polycyclic aromatic hydrocarbon epoxides, Chem. Res. Toxicol. 10 (1997) 880–886.
[3] X.M. He, D.C. Carter, Atomic structure and chemistry of human serum albumin, Nature 358 (1992) 209–215.
[4] T. Peters Jr., All About Albumin: Biochemistry, Genetics, Medical Applications, Academic Press, Academic Press, San Diego, 1995.
[5] G. Sudlow, D.J. Birkett, D.N. Wade, The characterization of two specific drug binding sites on human serum albumin, Mol. Pharmacol. 11 (1975) 824–832.
[6] A. Sengupta, D.S. Hage, Characterization of minor site probes for human serum albumin by high-performance affinity chromatography, Anal. Chem. 71 (1999) 3821–3827.
[7] F.A. de Wolf, G.M. Brett, Ligand-binding proteins: their potential for application in systems for controlled delivery and uptake of ligands, Pharmacol. Rev. 52 (2000) 207–236.
[8] J.K.A. Kamal, L. Zhao, A.H. Zewail, Ultrafast hydration dynamics in protein unfolding: human serum albumin, Proc. Natl. Acad. Sci. U.S.A. 101 (2004) 13411–13416.
[9] M. Roche, C. Dufour, M. Loonis, M. Reist, P.-A. Carrupt, O. Dangles, Olive phenols efficiently inhibit the oxidation of serum albumin-bound linoleic acid and butyrylcholine esterase, Biochim. Biophys. Acta – General Subjects 1790 (2009) 240–248.
[10] H.N. Bischel, L.A. MacManus-Spencer, R.G. Luthy, Noncovalent interactions of long-chain perfluoroalkyl acids with serum albumin, Environ. Sci. Technol. 44 (2010) 5263–5269.
[11] P.C. Hebert, L.A. MacManus-Spencer, Development of a fluorescence model for the binding of medium- to long-chain perfluoroalkyl acids to human serum albumin through a mechanistic evaluation of spectroscopic evidence, Anal. Chem. 82 (2010) 6463–6471.
[12] L.A. MacManus-Spencer, M.L. Tse, P.C. Hebert, H.N. Bischel, R.G. Luthy, Binding of perfluorocarboxylates to serum albumin: a comparison of analytical methods, Anal. Chem. 82 (2010) 974–981.
[13] S. Monti, I. Manet, F. Manoli, G. Marconi, Structure and properties of licochalcone A-human serum albumin complexes in solution: a spectroscopic, photophysical and computational approach to understand drug-protein interaction, Phys. Chem. Chem. Phys. 10 (2008) 6597–6606.
[14] G. Sudlow, D.J. Birkett, D.N. Wade, Spectroscopic techniques in the study of protein binding: the use of 1-anilino-8-naphthalenesulphonate as a fluorescent probe for the study of the binding of iophenoxic and iopanoic acids to human serum albumin, Mol. Pharmacol. 9 (1973) 649–657.
[15] J.R. Lakowicz, Principles of Fluorescence Spectroscopy, third ed., Springer Science+ Business Media, New York, 2006.
[16] A.N. Jain, Surflex:, Fully automatic flexible molecular docking using a molecular similarity-based search engine, J. Med. Chem. 46 (2003) 499–511.
[17] N.J. Greenfield, G.D. Fasman, Computed circular dichroism spectra for the evaluation of protein conformation, Biochemistry 8 (1969) 4108–4116.
[18] O.K. Abou-Zied, O.I.K. Al-Shihi, Characterization of subdomain IIA binding site of human serum albumin in its native, unfolded, and refolded states using small molecular probes, J Am. Chem. Soc. 130 (2008) 10793–10801.
[19] P.L. Gentili, F. Ortica, G. Favaro, Static and dynamic interaction of a naturally occurring photochromic molecule with bovine serum albumin studied by UV-visible absorption and fluorescence spectroscopy, J. Phys. Chem. B 112 (2008) 16793–16801.
[20] A. Divsalar, M.J. Bagheri, A.A. Saboury, H. Mansoori-Torshizi, M. Amani, Investigation on the interaction of newly designed anticancer Pd(II) complexes with different aliphatic tails and human serum albumin, J. Phys. Chem. B 113 (2009) 14035–14042.
[21] T. Banerjee, S.K. Singh, N. Kishore, Binding of naproxen and amitriptyline to bovine serum albumin: biophysical aspects, J. Phys. Chem. B 110 (2006) 24147–24156.
[22] D. Balbinot, S. Atalick, D.M. Guldi, M. Hatzimarinaki, A. Hirsch, N. Jux, Electrostatic assemblies of fullerene-porphyrin hybrids: toward long-lived charge separation, J. Phys. Chem. B 107 (2003) 13273–13279.
[23] B. Ahmad, M.Z. Ahmed, S.K. Haq, R.H. Khan, Guanidine hydrochloride denaturation of human serum albumin originates by local unfolding of some stable loops in domain III, Biochim. Biophys. Acta – Proteins & Proteomics 1750 (2005) 93–102.
[24] L. Galantini, C. Leggio, N.V. Pavel, Human serum albumin unfolding: A small-angle X-ray scattering and light scattering study, J. Phys. Chem. B 112 (2008) 15460–15469.
[25] L. Stryer, Fluorescence spectroscopy of proteins, Science 162 (1968) 526–533.
[26] G. Weber, E. Daniel, Cooperative effects in binding by bovine serum albumin. II. The binding of 1-anilino-8-naphthalenesulfonate. Polarization of the ligand fluorescence and quenching of the protein fluorescence, Biochemistry 5 (1966) 1900–1907.
[27] L. Stryer, The interaction of a naphthalene dye with apomyoglobin and apohemoglobin: a fluorescent probe of non-polar binding sites, J. Mol. Biol. 13 (1965) 482–495.
[28] L.A. Bagatolli, S.C. Kivatinitz, F. Aguilar, M.A. Soto, P. Sotomayor, G.D. Fidelio, Two distinguishable fluorescent modes of 1-anilino-8-naphthalenesulfonate bound to human albumin, J. Fluoresc. 6 (1996) 33–40.
[29] D.I. Cattoni, S.B. Kaufman, F.L.G. Flecha, Kinetics and thermodynamics of the interaction of 1-anilino-naphthalene-8-sulfonate with proteins, Biochim. Biophys. Acta – Proteins & Proteomics 1794 (2009) 1700–1708.
[30] A. Hawe, R. Poole, W. Jiskoot, Misconceptions over Förster resonance energy transfer between proteins and ANS/bis-ANS: direct excitation dominates dye fluorescence, Anal. Biochem. 401 (2010) 99–106.
[31] D.C. Carter, J.X. Ho, Structure of serum albumin, Adv. Protein Chem. 45 (1994) 153–203.
[32] J. Ghuman, P.A. Zunszain, I. Petitpas, A.A. Bhattacharya, M. Otagiri, S. Curry, Structural basis of the drug-binding specificity of human serum albumin, J. Mol. Biol. 353 (2005) 38–52.
[33] I. Sjöholm, B. Ekman, A. Kober, I. Ljungstedt-Påhlman, B. Seiving, T. Sjödin, Binding of drugs to human serum albumin:XI.[1] The specificity of three binding sites as studied with albumin immobilized in microparticles[2], Mol. Pharmacol. 16 (1979) 767–777.
[34] D. Russo, J. Ollivier, J. Teixeira, Water hydrogen bond analysis on hydrophilic and hydrophobic biomolecule sites, Phys. Chem. Chem. Phys. 10 (2008) 4968–4974.

[35] A. Sułkowska, Interaction of drugs with bovine and human serum albumin, J. Mol. Struct. 614 (2002) 227–232.
[36] N.J. Greenfield, Determination of the folding of proteins as a function of denaturants, osmolytes or ligands using circular dichroism, Nat. Protoc. 1 (2006) 2733–2741.
[37] J.S Mandeville, H.-A. Tajmir-Riahi, Complexes of dendrimers with bovine serum albumin, Biomacromolecules 11 (2010) 465–472.
[38] D.M. Charbonneau, H.-A. Tajmir-Riahi, Study on the interaction of cationic lipids with bovine serum albumin, J. Phys. Chem. B 114 (2010) 1148–1155.